

Nitrification Modeling in Chloraminated Distribution Systems

Suibing Liu

*James S. Taylor

A. A. Randall

John D. Dietz

Department of Civil and Environmental Engineering
University of Central Florida

P.O. BOX 162450, Orlando, FL, 32816-2450, USA

*Corresponding author: Tel (407)823-2785, Fax (407)823-3315, E-mail: taylor@mail.ucf.edu

Abstract

This paper describes a kinetic model for nitrification in a drinking water distribution system. Using *Monod kinetics*, a steady state plug-flow kinetics model was developed to describe the variations of ammonia, nitrite and nitrate-N concentrations in a chloraminated distribution system. Active AOB and NOB biomass in the distribution system was determined using predictive equations within the model. The kinetic model used numerical analysis and was solved by C language to predict ammonia, nitrite, nitrate variation.

Introduction

Biochemical nitrification probably exists to some degree in every distribution system using chloramines. Although violations of the nitrate-N regulation is rarely if ever heard of in drinking water distribution systems, modeling biochemical nitrification is beneficial for proactive control of distribution system water quality. Chloramination has been implemented by many utilities in the United States, for residual and disinfection by-product (DBP) control (Wolfe *et al*, 1985, LeChevallier, 1990, Ollos, 1998, Jegatheesan, 2000; AWWA & AWWARF, 1990, Brodtmann, 1979; Mitcham, 1983; Hack, 1984; Valentine, 1986; Lykins, 1994; Leung, 1994; Thomas, 1987; Taylor, 1986).

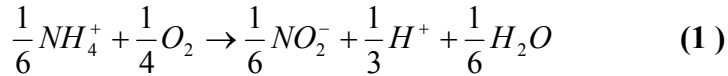
The EPA accepted monochloramine as a secondary disinfectant in 1978, and as a primary disinfectant in 1983 (White, 1999). Nitrification has been reported in some systems using monochloramine (Barrios, 1989; Wolfe, 1988 and 1990; Cunliffe, 1991; Lieu 1993) and was also observed with blending of different source waters in reservoirs. Sixty-three percent of these utilities experienced nitrification (Wilczak, 1996, Odell, 1996). One analytical survey of five chloraminated distribution systems in South Australia showed that sixty four percent of distribution system samples tested positive for nitrifying bacteria (Cunliffe, 1991, Regan, 2002). A high chloramines residual in treatment plant effluent may not prevent nitrification (Wilczak *et. al* 1996). Nitrification has been shown to occur at monochloramine concentrations of more than 5.0 mg/L

(Cunliffe 1991). Biochemical nitrification has been observed in a drinking water distribution system at high chloramines concentrations (3-6 mg/L) in finished water, (Wilczak et. al 1996).

Nitrification of ammonia is a two-step biochemical process in which ammonia is oxidized to nitrite, and then nitrite is further oxidized to nitrate. Two groups of chemoautotrophic bacteria, namely ammonia-oxidizing-bacteria (AOB) and nitrite-oxidizing bacteria (NOB) are thought to utilize ammonia and nitrite respectively as their energy sources (Lieu et al. 1993, Skadsen 1993, Wolfe et al. 1988).

Nitrosomonas bacteria oxidize ammonia to nitrite, while *Nitrobacter* bacteria convert nitrite to nitrate, with both species utilizing the energy released from the reactions. The reactions involved are complicated, but can be summarized as shown in Equations (1) and (2) (Grady, Daigger and Lim 1999).

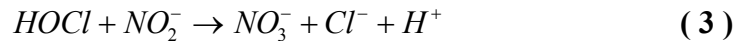
For AOB nitrification:



For NOB nitrification:



Furthermore, nitrite, the product from the AOB growth, rapidly reduces free chlorine (Rittmann and Snoeyink 1984) and accelerates the chloramine decomposition in a redox reaction forming nitrates (Valentine 1984). Wolfe et al. (1988) showed that a chlorine demand of 5 mg/L is exerted by 1 mg/L of NO₂-N. The reactions involved are presented in Equations (3) and (4) (Chen, 2001).



The most frequently used kinetic equation for representing bacterial growth is the *Monod equation* (Rittmann, 2001), which is shown in Equation (5):

$$\mu_{syn} = \left(\frac{1}{X_a} \frac{dX_a}{dt} \right)_{syn} = \hat{\mu} \frac{S}{K + S} \quad (5)$$

Where μ_{syn} : specific growth rate due to synthesis (T^{-1})
 X_a : concentration of active biomass (M_xL^{-3})
 t : time (T)
 S : concentration of the rate limiting substrate (M_sL^{-3})
 $\hat{\mu}$: maximum specific growth rate (T^{-1})
 K : concentration giving one-half the maximum rate (M_sL^{-3})

The rate of substrate utilization is often described using the same type of equation as for the rate of bacterial growth. The form of the *Monod* equation for substrate utilization is shown in Equation (6).

$$r_{ut} = -\frac{\hat{q}S}{K+S}X_a \quad (6)$$

Where r_{ut} : rate of substrate utilization ($M_sL^{-3}T^{-1}$)
 \hat{q} : maximum specific rate of substrate utilization ($M_sM_x^{-1}T^{-1}$)

The relation between biomass growth and substrate utilization is quantitatively shown in Equation (7).

$$\hat{\mu} = \hat{q}Y \quad (7)$$

Where Y : true yield for cell synthesis ($M_xM_s^{-1}$)

Incorporation of this relationship into the rate of substrate utilization yields the net cell growth as shown in Equation (8).

$$r_{net} = \mu X_a = Y \frac{\hat{q}S}{K+S} X_a - bX_a \quad (8)$$

Where r_{net} : the net rate of active-biomass growth ($M_sL^{-3}T^{-1}$)
 μ : net specific growth rate of active biomass (T^{-1})
 b : endogenous-decay coefficient (T^{-1})

The rates of microbial growth can be slowed by the presence of inhibitory compounds (Rittmann, 2001), such as disinfectants. Self-inhibition is when the enzyme catalyzed degradation of the substrate is slowed by high concentrations of the substrate, which is represented quantitatively in Equation (9).

$$\hat{q}_{eff} = \frac{\hat{q}}{1 + \frac{S}{K_{IS}}} \quad \text{or} \quad K_{eff} = \frac{K}{1 + \frac{S}{K_{IS}}} \quad (9)$$

Where \hat{q}_{eff} : effective maximum specific rate of substrate utilization ($M_sM_x^{-1}T^{-1}$)
 K_{eff} : effective concentration giving one-half the maximum rate (M_sL^{-3})
 K_{IS} : inhibition concentration of self-inhibitory substrate (M_sL^{-3})

If more than one substrate is rate limiting, which is typical and referred to as dual limitation, the rate of bacterial growth can be written as Equation (10).

$$r_{ut} = -\frac{\hat{q}S}{K+S} \frac{A}{K_A+A} X_a \quad (10)$$

Where A : concentration of the rate limiting substrate A (M_sL^{-3})
 K_A : concentration giving one-half the maximum rate for substrate A (M_sL^{-3})

Vayenas et al. (1997) developed a dynamic model describing nitrification in trickling filters. The model predicted the concentration profiles of ammonia, nitrite and nitrate along the filter depth and along the biofilm depth, as a function of the operating parameters, in batch and continuous operation. The model also predicted the biofilm thickness as a function of filter depth and time. No disinfectant inhibition or dissolved oxygen limitation were considered in the model. The continuous version of the model was verified by pilot-scale experiments and states that nitrite accumulation would be observed only when a significant ammonia concentration was observed at the filter outlet.

Lu et al. (1995) developed a mathematical model that accounts for simultaneous transport of substrates, disinfectants and microorganisms to predict substantial changes in the quality of distributed drinking water. The model consisted of a set of mass balance equations for organic substances, ammonium nitrogen, oxidized nitrogen, dissolved oxygen, alkalinity, biomass, and disinfectants in the bulk liquid phase and within the biofilm under both laminar and turbulent flow conditions. The model was validated by comparing model solutions with numerical solutions in the literature, and was then applied for predicting the behavior of a typical water treatment plant effluent through a distribution pipe. The flow properties and disinfectant (free chlorine) consumption rate at the pipe wall played a significant role in the determination of potable water quality in the distribution system.

Chandran and Smets (2000) formulated a mechanically based nitrification model to determine $\text{NH}_4\text{-N}$ to $\text{NO}_2\text{-N}$ and $\text{NO}_2\text{-N}$ to $\text{NO}_3\text{-N}$ oxidation kinetics from a single $\text{NH}_4\text{-N}$ to $\text{NO}_3\text{-N}$ batch-oxidation profile by explicitly considering the kinetics of each oxidation step. In the model, stoichiometric coefficients relating nitrogen removal, oxygen uptake, and biomass synthesis were derived from an electron-balanced equation. A parameter identifying analysis of the developed two-step model revealed a decrease in correlation and an increase in the precision of the kinetics parameter estimates when $\text{NO}_2\text{-N}$ oxidation kinetics became increasingly rate-limiting. These findings demonstrate that two-step models describe nitrification kinetics adequately only when $\text{NH}_4\text{-N}$ to $\text{NO}_3\text{-N}$ oxidation profiles contain sufficient information pertaining to both nitrification steps. Thus, the rate-determining step in overall nitrification must be identified before applying conventionally used models to describe batch nitrification respirograms.

Tsuno et al. (2002) developed a simple biofilm model of competition in bacterial growth for an attached surface. Competition for the attached surface was expressed with crowded and detachment effects. The developed model was verified by comparing simulated results with data obtained in experiments with batch culture of nitrifiers and continuous treatment of actual sewage in a biofilm reactor. The model favorably simulated the growth competition between autotrophic and heterotrophic bacteria for the attached surface. Interpretation of the model showed effective nitrification in the biofilm reactor required removal of organic matter before the nitrification tank (Tsuno et al. 2002).

Chandran and Smets (2001) derived expressions for biomass yield coefficients describing autotrophic ammonia and nitrite oxidation from a mechanistically based

electron balanced equation. They demonstrated that applying the conventional expression used to calculate the heterotrophic biomass yield results in erroneous estimates for the autotrophic biomass yield and the yield coefficients for autotrophic $\text{NH}_4\text{-N}$ to $\text{NO}_2\text{-N}$ oxidation and $\text{NH}_4\text{-N}$ to $\text{NO}_3\text{-N}$ oxidation are overestimated by 27 to 36 percent. Due to correlation between the maximum specific growth rate and the biomass yield, a 30 to 40 percent error in yield values results in an overestimate of the maximum specific growth rate coefficient for $\text{NH}_4\text{-N}$ oxidation determined from batch respirograms. Therefore, it is essential to employ the correct expression to estimate the autotrophic biomass yield coefficient from batch respirograms due to its inadvertent impact on subsequent parameter estimation.

Although substantial work has been done on modeling of microbial activity in water treatment systems, only a few mathematical models describe nitrification in the drinking water distribution systems. The substrate concentration (ammonia or nitrite) is lower than substrate concentrations in biofilters or bioreactors, and monochloramines inhibit bacterial growth both of which makes modeling microbiological activity in drinking water distribution systems more difficult than in wastewater systems.

Pilot Plant Design

Waters were produced from seven different treatment systems shown in Table 1 (Taylor et al. 2001, Liu et al. 2003). The RO source was augmented with salts to mimic seawater. The pilot process water tanks are shown in Figure 1. The finished waters were blended and distributed to 18 different pilot distribution systems (PDS) shown in Figure 2.

Table 1 Pilot Plant Treatment Systems

Identification	Source Water	Treatment Processes
G1	Groundwater	Aeration, Disinfection, pH stabilization
G2	Groundwater	Softening, Sedimentation, Filtration, Disinfection, pH stabilization
G3	Groundwater, RO and S1 Blends *	Softening, Sedimentation, Filtration and Disinfection, pH stabilization
G4	Groundwater, RO and S1 Blends *	Nano-filtration, Disinfection, pH stabilization
S1	Surface Water	Coagulation, Sedimentation, Filtration, (CSF) Ozone, BAC, Filtration, Disinfection, pH stabilization
S2	Surface Water	Coagulation, Flocculation, Sedimentation, Nano-filtration, Disinfection, pH stabilization
RO	Groundwater	5 μm cartridge pre-filtration, RO, Disinfection, pH stabilization

* The groundwater, S1 and RO blend ratio was 60%:30%:10%.



Figure 1 Process Water Tanks

There were 18 pilot distribution systems (PDSs). The PDSs consisted of PVC, galvanized steel (G), lined cast iron (LCI) and unlined cast iron (UCI) pipes taken from existing distribution systems. Fourteen of the PDSs were hybrid lines, consisting of PVC, LCI, UCI, and G pipes in that order. Four PDSs were totally either PVC, LCI, UCI or G pipes and are described as single material lines (Taylor 2001, Liu et al. 2003).



Figure 2 Distribution System of Pilot Plant

The duration of the pilot plant operations was one and one-half years. The period of operation discussed in this work is from 9/13/2002 to 12/14/2002, when nitrification occurred in the PDSs. The PDS hydraulic resident time (HRT) was 2 days during this period.

Model Building

The development of the model was based on the following:

1. The flow in the pipes was treated as plug flow, since the length of the pipe is much larger than the diameter. Hence plug flow based mass balance can be used to describe the PDSs.
2. The biofilm thickness on the pipe wall was very small relative to the diameter of the pipe (6"), the biofilm effect was not as strong as in a biofilm reactor, consequently, the bioactivity in the biofilm was combined into and represented by the combined bulk water bioactivity and associated bio-parameters.
3. Ammonia consisted of free ammonia in the PDS feed stream and ammonia released from the decomposition of chloramines.
4. Monochloramine, ammonia, nitrite and nitrate were transported parallel to the pipe surface.
5. Biological growth was limited by ammonia, D.O. and nitrite and could be described by *Monod* kinetics.
6. Biomass growth was non-competitively inhibited by chloramines.
7. The pipe was divided into segments, and numerical analysis was used for mass balances of each segment.
8. No denitrification occurred in the system.

The specific growth rates for AOB and NOB were given by *Monod* kinetics and included D.O. limitation and the residual inhibition as shown in Equations (11) and (12).

$$\mu_{(C_{NH_3i})} = \frac{\hat{\mu}_{1\max} C_{NH_3i}}{K_{NH_3} + C_{NH_3i}} \left(\frac{1}{1 + \frac{C_{NH_2Cl_i}}{K_{NH_2Cl}}} \right) \cdot \left(\frac{DO_i}{K_{O_2} + DO_i} \right) \quad (11)$$

$$\mu_{(C_{NO_2i})} = \frac{\hat{\mu}_{2\max} C_{NO_2i}}{K_{NO_2} + C_{NO_2i}} \left(\frac{1}{1 + \frac{C_{NH_2Cl_i}}{K_{NH_2Cl}}} \right) \cdot \left(\frac{DO_i}{K_{O_2} + DO_i} \right) \quad (12)$$

Where C_{NH_3i} : ammonia concentration at i^{th} segment (mg/cm^3 as N)
 C_{NO_2i} : nitrite concentration at i^{th} segment (mg/cm^3 as N)
 $C_{NH_2Cl_i}$: monochloramine concentration at i^{th} segment (mg/cm^3 as Cl_2)
 DO_i : dissolved oxygen concentration at i^{th} segment (mg/cm^3)
 $\mu_{(C_{NH_3i})}$: specific growth rate of AOB at i^{th} segment (day^{-1})
 $\mu_{(C_{NO_2i})}$: specific growth rate of NOB at i^{th} segment (day^{-1})
 K_{NH_2Cl} : inhibition concentration of monochloramine (mg/cm^3 as Cl_2)
 K_{NH_3} : ammonia concentration giving one-half the AOB maximum rate (mg/cm^3 as N)
 K_{NO_2} : nitrite concentration giving one-half the NOB maximum rate (mg/cm^3 as N)
 K_{O_2} : oxygen concentration giving one-half the AOB and NOB maximum rate (mg/cm^3)
 $\hat{\mu}_{1\max}$: maximum specific growth rate of AOB (day^{-1})
 $\hat{\mu}_{2\max}$: maximum specific growth rate of NOB (day^{-1})

Subscript i : the effluent of i^{th} segment, or the influent of $(i+1)^{\text{th}}$ segment

The first part of the right hand side (RHS) of equations (11) and (12) is the normal *Monod* expression with ammonia or nitrite as the substrate, the second part of the RHS of equations (11) and (12) considers the inhibition effect of monochloramine, and the third part of equations (11) and (12) considers the limiting effect of dissolved oxygen.

Mass balances for ammonia, nitrite and nitrate at the bulk liquid, at the i^{th} segment of the pipe, are shown in Equation (13), (14) and (15).

$$0 = \frac{1}{HRT_i} (C_{NH_3(i-1)} - C_{NH_3i}) - \frac{1}{Y_{X_1}} \mu_{(C_{NH_3i})} X_1 + \frac{1}{HRT_i} (C_{NH_2Cl(i-1)} - C_{NH_2Cl_i}) \quad (13)$$

Where Subscript $(i-1)$: the effluent of $(i-1)^{\text{th}}$ segment, or the influent of i^{th} segment
 X_1 : concentration of AOB active biomass (mg VSS/cm³)
 Y_{X_1} : true yield of AOB for cell synthesis (mg VSS/mg NH₃-N)
 HRT_i : hydraulic residence time of i^{th} segment in the pipe (Day)

The first term of the RHS of Equation (13) represents the ammonia difference between the inlet and the outlet concentrations in the bulk liquid in the i^{th} segment of the pipe, the second term of the RHS of Equation (13) represents the degradation of ammonia by AOB, and the third term of the RHS of Equation (13) represents the release of ammonia from monochloramine decomposition. Since it was assumed that the system was at steady state, the LHS of Equation (13) was zero.

$$0 = \frac{1}{HRT_i} (C_{NO_2(i-1)} - C_{NO_2i}) + \frac{1}{Y_{X_1}} \mu_{(C_{NH_3i})} X_1 - \frac{1}{Y_{X_2}} \mu_{(C_{NO_2i})} X_2 \quad (14)$$

Where Y_{X_2} : true yield of NOB for cell synthesis (mg VSS/mg NO₂-N)
 X_2 : concentration of NOB active biomass (mg VSS/cm³)

The first term in the RHS of Equation (14) represents the nitrite difference between the inlet and the outlet concentrations in the bulk liquid in the i^{th} segment of the pipe, the second term in the RHS of Equation (14) represents the generation of nitrite by AOB, and the third term in the RHS of Equation (14) represents the consumption of nitrite by NOB. Zero for the LHS of Equation (14) represents a steady state system.

$$0 = \frac{1}{HRT_i} (C_{NO_3(i-1)} - C_{NO_3i}) + \frac{1}{Y_{X_2}} \mu_{(C_{NO_2i})} X_2 \quad (15)$$

Zero for the LHS of Equation (15) represents a steady state system. The first term of the RHS of Equation (15) represents the nitrate difference between the inlet and the

outlet concentrations in the bulk liquid in the i^{th} segment of the pipe, and the second term of Equation (15) represents the generation of nitrate by NOB.

The initial conditions were that the concentrations of D.O., ammonia, nitrite, nitrate and monochloramine of the first segment of the pipe were equal to those of the influent water as defined in Equations (16), (17), (18), and (19).

$$C_{NH_3i0} = C_{NH_3entrance} \quad (16)$$

Where C_{NH30} : initial influent concentration for ammonia of first segment (mg/cm^3 as N)
 $C_{NH3entrance}$: ammonia concentration entering PDS (mg/cm^3 as N)

$$C_{NO_20} = C_{NO_2entrance} \quad (17)$$

Where C_{NO20} : initial influent concentration for nitrite of first segment (mg/cm^3 as N)
 $C_{NO2entrance}$: nitrite concentration entering PDS (mg/cm^3 as N)

$$C_{NO_30} = C_{NO_3entrance} \quad (18)$$

Where C_{NO30} : initial influent concentration for nitrate of first segment (mg/cm^3 as N)
 $C_{NO3entrance}$: nitrate concentration entering PDS (mg/cm^3 as N)

$$C_{NH_2Cl0} = C_{NH_2Clentrance} \quad (19)$$

Where C_{NH2Cl0} : initial influent concentration for nitrate of first segment (mg/cm^3 as N)
 $C_{NH2Clentrance}$: nitrate concentration entering PDS (mg/cm^3 as N)

Because it is assumed that no denitrification occurred in the PDSs, and the organic nitrogen influence was ignored, the total nitrogen balance is described by Equation (20).

$$\begin{aligned} C_{NH_3i} + C_{NO_2i} + C_{NO_3i} + C_{NH_2Cl_i} \\ = C_{NH_30} + C_{NO_20} + C_{NO_30} + C_{NH_2Cl0} \end{aligned} \quad (20)$$

Parameter Estimation

Most of the kinetics parameters and constants required in the model could not be determined in the experiment. However, the parameters are unique to the AOB and NOB bacteria and can be taken from the literature. The selected kinetic parameters and constants are shown with references in Table 2.

Table 2 Kinetics Parameters and Constants Values

Parameter	Unit	Model Value	Reference
K_{NH_2Cl}	(mg/cm ³ as Cl ₂)	0.0005	Estimation from the field data
K_{NH_3}	(mg/cm ³ as N)	0.0002	Antonious, 1989
K_{NO_2}	(mg/cm ³ as N)	0.0012	Metcalf and Eddy, 1991
K_{O_2}	(mg/cm ³)	0.0004	Williamson and McCarty, 1976
$\hat{\mu}_{1max}$	(day ⁻¹)	0.4	Antonious, 1989
$\hat{\mu}_{2max}$	(day ⁻¹)	0.55	Metcalf and Eddy, 1991
Y_{X1}	(mg VSS/mg NH ₃ -N)	0.19	Metcalf and Eddy, 1991
Y_{X2}	(mg VSS/mg NO ₂ -N)	0.10	Poduska and Andrews, 1974

It should be noted that some kinetics parameters and constant were temperature dependent, such as $\hat{\mu}_{1max}$, $\hat{\mu}_{2max}$, K_{NH_3} , and K_{NO_2} . But the temperature in this pilot study was not controllable, which is also the case for the real distribution systems. The daily temperature variation in the PDSs was from 18 to 30 °C approximately. Consequently, the temperature effect was not considered separately for each parameters or constants, but as discussed later, the active biomass concentrations estimated from the field data reflected the temperature effect as a whole.

As shown in Figure 3, when the combined residual in the PDS was above 1.0 mg/L as Cl₂, nitrification was significantly reduced because AOB growth was inhibited. The chlorine inhibition coefficient as shown in Equations (11) and (12) was set as the average of the range of chloramine concentrations where the majority of nitrification occurred. This range was 0 to approximately 1 mg/L as Cl₂, consequently the chlorine inhibition coefficient was 0.5 mg/L as Cl₂ (0.0005 mg/cm³).

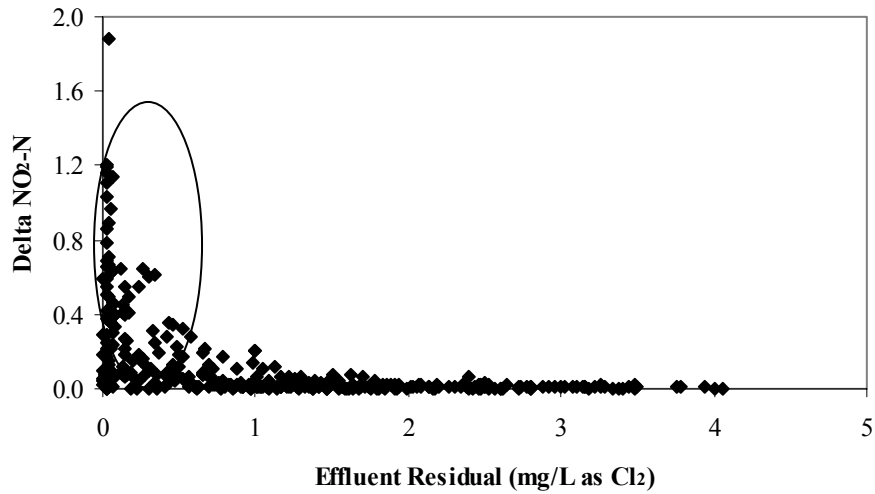


Figure 3 Monochloramine Residual Effect on Nitrification

The AOB and NOB active biomass concentrations were unique to the systems and were indirectly determined from field observations. The AOB biomass was determined using Equation (11), Equation (13) and the actual ammonia, chlorine, and DO for each increment. Incremental AOB biomass was averaged for general model use.

The actual chlorine, nitrite, ammonia, and DO were used in Equations (12) and (14) to determine incremental NOB biomass, which was averaged to determine X_2 for general equation use.

X_1 and X_2 generally increased with temperature and were fitted to an exponential equation as shown in Figure 4. The development of the model did not consider nitrite oxidation by chloramines separately but combined chemical and biological nitrite oxidation into a single term.

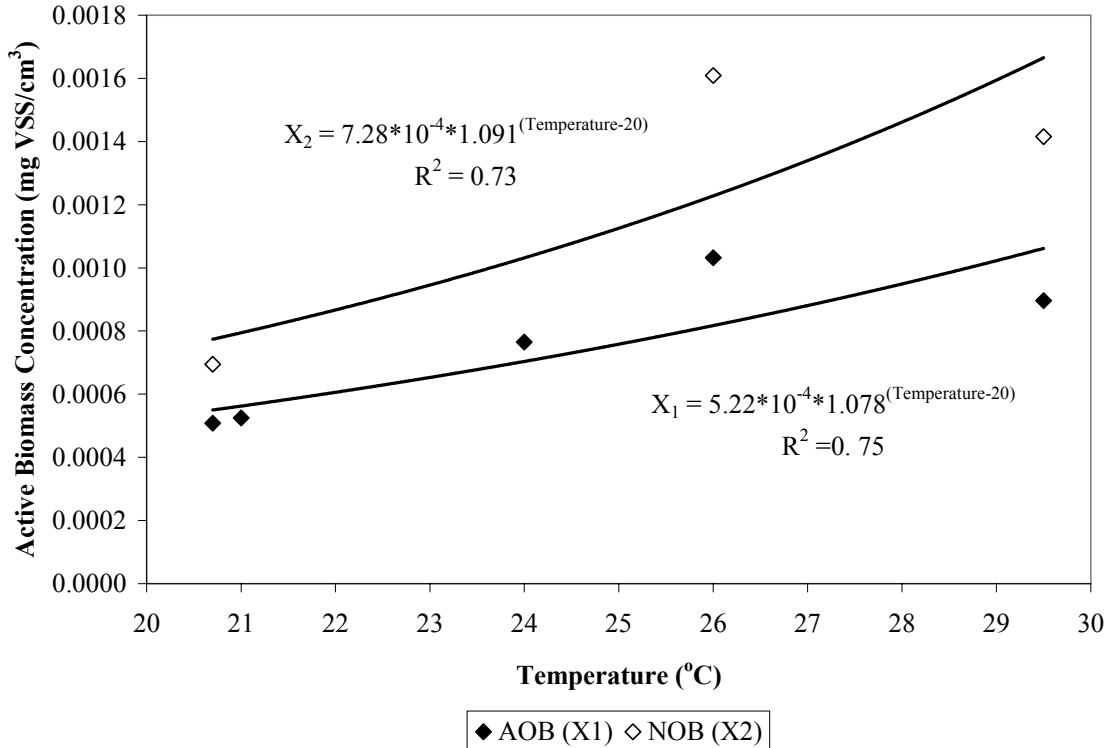


Figure 4 Correlation of AOB (X₁) and NOB (X₂) Active Biomass Concentration with Temperature

Consequently, the equation used to predict AOB and NOB active biomass in the distribution system is shown as Equation (21), and (22) respectively:

$$X_1(\text{mgVSS} / \text{cm}^3) = 5.22 \times 10^{-4} \times 1.078^{(\text{Temperature}-20^\circ \text{C})} \quad (21)$$

$$X_2(\text{mgVSS} / \text{cm}^3) = 7.28 \times 10^{-4} \times 1.091^{(\text{Temperature}-20^\circ \text{C})} \quad (22)$$

The temperatures of the PDSs were rarely above 35 °C. When the temperature was below 15 °C, the nitrification was usually not an issue in the PDSs (Lieu, 1993). Consequently, the suitable temperature range for Equation (21) and (22) is 15-35 °C. The predicted X₁ and X₂ for this work are presented in Table 3:

Table 3 Active AOB (X₁) and NOB (X₂) Biomass Concentration Prediction

Date	Temperature °C	X ₁ mg VSS/cm ³	X ₂ mg VSS/cm ³
10/10/02	29.5	0.0011	0.0016
10/25/02	26.0	0.0008	0.0012
11/08/02	20.7	0.0006	0.0007
11/22/02	24.0	0.0007	0.0010
12/06/02	21.0	0.0006	0.0008

The typical literature values of trickling filters in the drinking water treatment for X_1 and X_2 were 17 and 34 VSS mg/cm³ (Vayenas et al., 1997), and Rittmann et al. (2001) provided that the biomass concentration for active sludge nitrification system was about 1 VSS mg/cm³, and 10 VSS mg/cm³ for biofilm system. But in this distribution system, the calculated X_1 and X_2 ranges were 0.0006-0.0011 and 0.0007-0.0016 VSS mg/cm³ respectively. As expected, the active biomass concentrations were much lower than those in biological nitrification reactors treating drinking water or wastewater.

Model Prediction

Ammonia, nitrite and nitrate were predicted using the models previously discussed and the data from the unlined cast iron distribution system during October 2002 to December 2002. Predicted and actual ammonia, nitrite and nitrate are shown in Figure 5 to Figure 9.

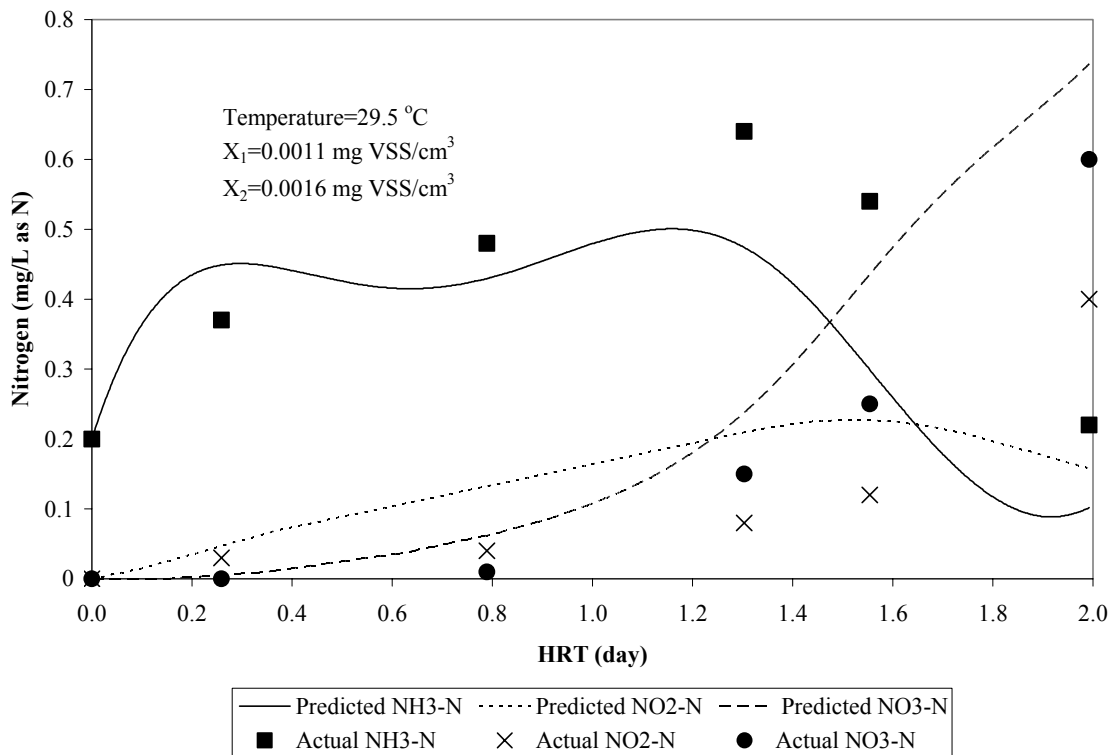


Figure 5 Bulk Water Profiles with HRT in the UCI PDS (Date 10/10/02)

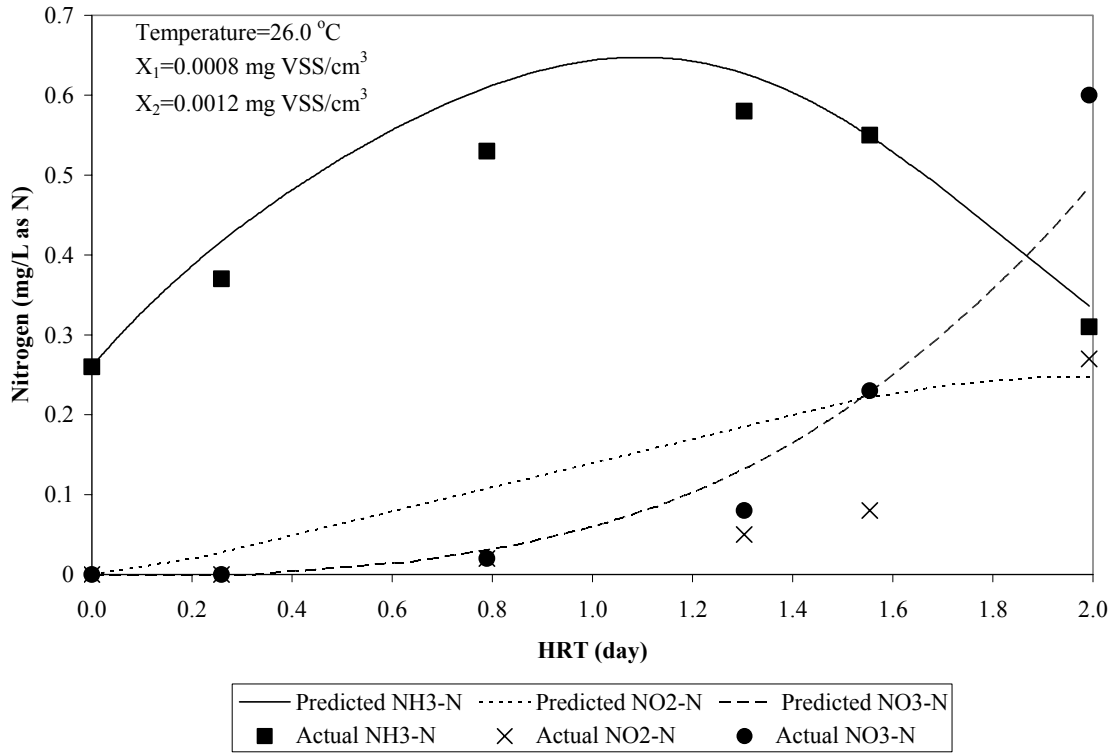


Figure 6 Bulk Water Profiles with HRT in the UCI PDS (Date 10/25/02)

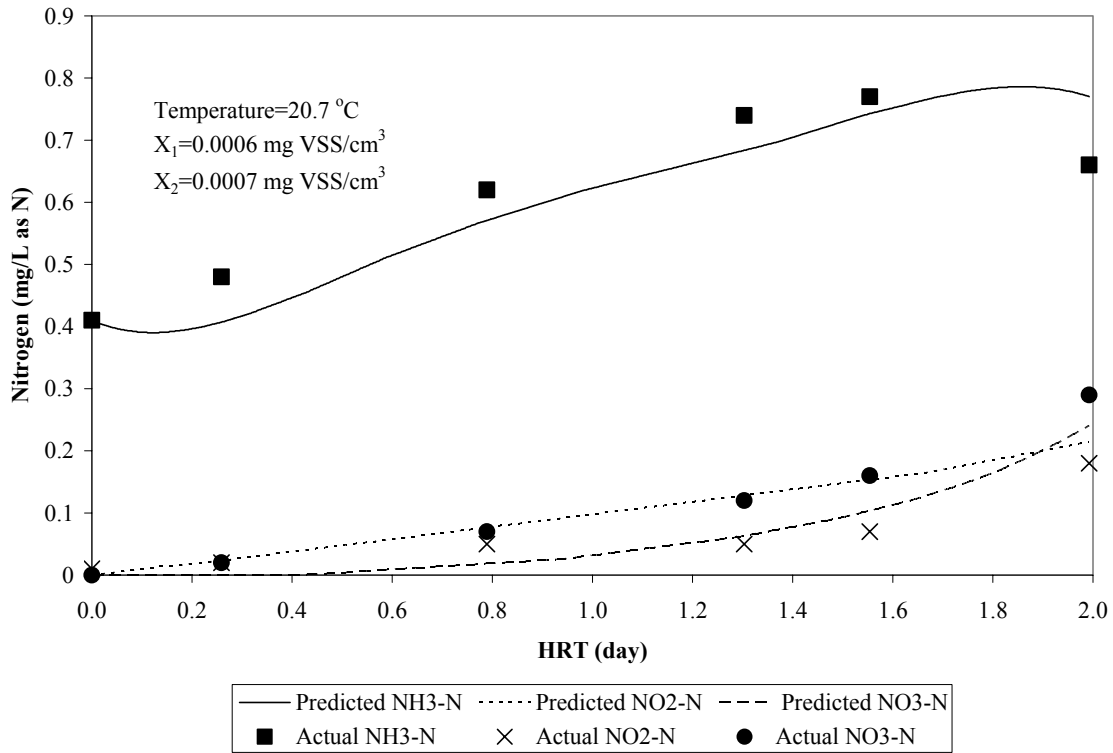


Figure 7 Bulk Water Profiles with HRT in the UCI PDS (Date 11/08/02)

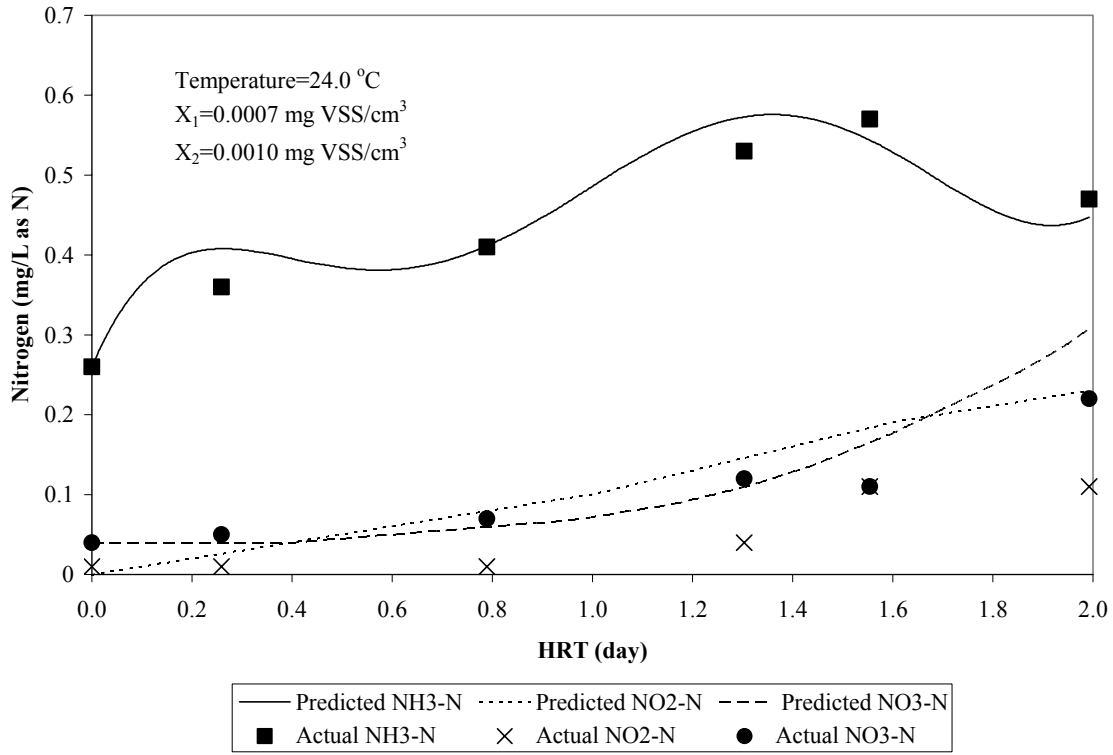


Figure 8 Bulk Water Profiles with HRT in the UCI PDS (Date 11/22/02)

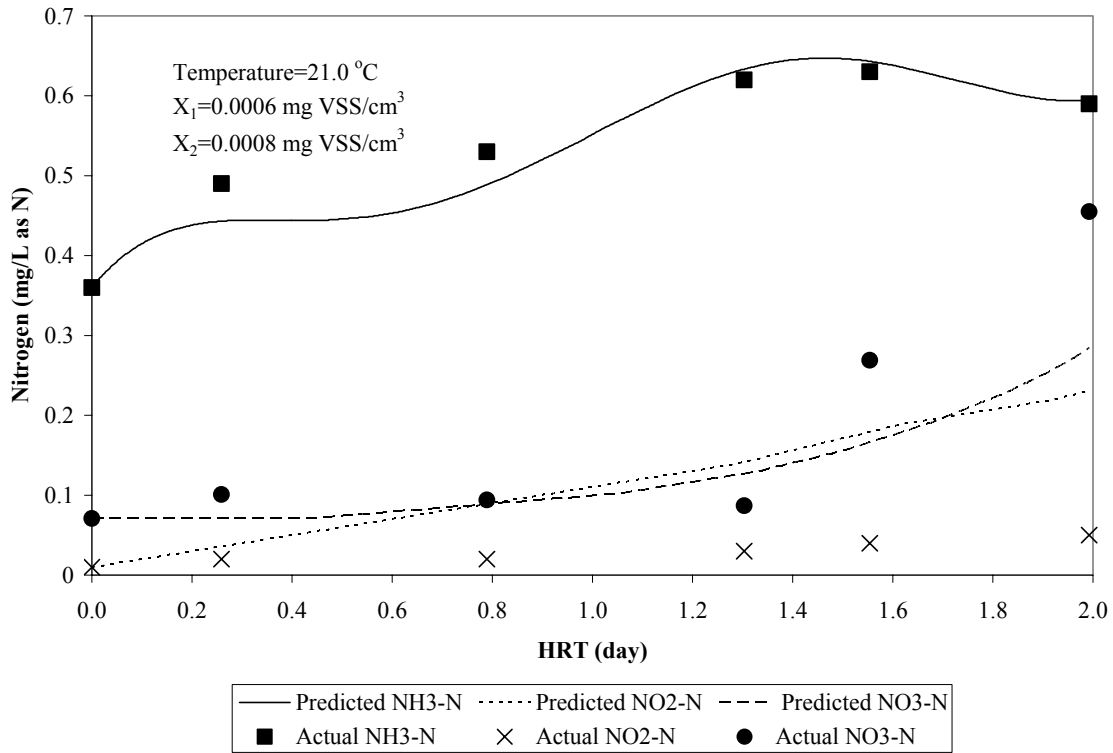


Figure 9 Bulk Water Profiles with HRT in the UCI PDS (Date 12/06/02)

As presented in the figures, the predicted nitrate concentrations are very close to that of the measured data. The predicted ammonia also followed the actual ammonia trend. But nitrite was over predicted for most observations.

There were a total of five sampling events at different dates from October to December 2002. For those sampling events, the measured nitrogen species showed different trends. Ammonia increased, decreased, increased and decreased on 10/10/02, 11/22/02, and 12/06/02 data creating a two peak trend. Ammonia only showed a one peak trend on 10/25/02 and 11/08/02. The peak was at the end of the pipe on 11/08/02. However the ammonia trend could be predicted by the model given the variation of the AOB biomass coefficient.

The predicted nitrate concentration represented the actual nitrate adequately. On 12/06/02, the actual nitrate varied significantly, which may have been due to sampling errors, analytical errors or anomalies within the PDS. The actual samples taken from the internal ports did not exactly represent the same increment of water as these samples were collected almost simultaneously and the PDS HRT was two days.

Nitrite was overestimated across the PDSs. This could be because nitrite oxidation to nitrate by chloramines which was not separately represented by the model. Inclusion of a specific chloramine oxidation of nitrite term may enhance accuracy of nitrite prediction.

Conclusions

- Monochloramine decomposed in distribution systems to produce free ammonia, and provided a nitrogen source for AOB and NOB growth and nitrite and nitrate production. Such trends were observed in this study.
- A steady state plug-flow model that predicted ammonia, nitrite and nitrate in a drinking water distribution system in presence of chloramines was developed using *Monod kinetics*.
- A model was developed for prediction of active AOB and NOB biomass in drinking water distribution systems. The independent variables were temperature, time, ammonia, chloramines and DO. The NOB model considered nitrite as well.
- The model predicted ammonia and nitrate concentrations adequately but overestimated nitrite, which may have been caused by the lack of consideration of nitrite oxidation by chloramines.
- The biokinetic parameter values developed for the model were selected from the literature. As expected, the calculated AOB and NOB active biomass concentrations were much lower than those in biological nitrification reactors.

Acknowledgment

Support for this research was provided by Tampa Bay Water (TBW), and AWWA Research Foundation (AWWARF). The authors are grateful to the project coordinator Chris Owens from TBW, Project officer Roy Martinez from AWWARF. In addition, the

authors thank the member governments of Pinellas County, Hillsborough County, Pasco County, Tampa, St. Petersburg, and New Port Richey.

References

- Antonius, P. 1989. Determination of biokinetic coefficients for nitrification in the activated sludge process. M. E. Thesis, Department of Environmental Engineering Sciences, University of Florida, Gainesville, FL.
- AWWA and AWWARF. 1990. Water Industry Data Base. AWWA and AWWARF, Denver, CO.
- Barrios, M.R., and P. Stone. 1989. Chloramine Depletion in Covered Reservoirs. Proceedings of AWWA WQTC. AWWA, Philadelphia, Pa.
- Brodthmann, N.V.J., and P.J. Russo. 1979. Use of Chloramine for Reduction of Trihalomethanes and Disinfection of Drinking Water. Journal of American Water Works Association, 71(1):40-42.
- Chandran, K., and B.F. Smets. 2000. Applicability of Two-step Models in Estimating Nitrification Kinetics from Batch Respirograms under Different Relative Dynamics of Ammonia and Nitrite Oxidation. Biotechnology and Bioengineering, 70(1):54-64.
- Chandran, K., and B.F. Smets. 2001. Estimating Biomass Yield Coefficients for Autotrophic Ammonia and Nitrite Oxidation from Batch Respirograms. Water Research, 35(13):3153-3156.
- Chen, W.-L., and J.N. Jensen. 2001. Effect of Chlorine Demand on the Ammonia Breakpoint Curve: Model Development, Validation with Nitrite, and Application to Municipal Wastewater. Water Environment Research, 73(6):721-731.
- Cunliffe, D.A. 1991. Bacterial Nitrification in Chloraminated Water Supplies. Applied and Environmental Microbiology, 57:3399-3402.
- Haas, C.N. 2000. Disinfection. R.D. Letterman, editor. In Water Quality & Treatment, A Handbook of Community Water Supplies, 5th edition. McGraw-Hill, Inc., New York.
- Hack, D.J. 1984. State Regulation of Chloramination. Journal of American Water Works Association, 77(1):46-49.
- Jegatheesan, V., G. Kastl, I. Fisher, M. Angles, and J. Chandy. 2000. Modeling Biofilm Growth and Disinfectant Decay in Drinking Water. Water Science and Technology, 41(4):339-345.
- Kirmeyer, G.J., L.H. Odell, J. Jacangelo, A. Wilczak, and R. Wolfe. 1995. Nitrification Occurrence and Control in Chloraminated Water Systems. AWWA Research Foundation, Denver, CO.
- LeChevallier, M.W., C.D. Lowry, and R.G. Lee. 1990. Disinfecting Biofilms in a Model Distribution System. Journal of American Water Works Association, 82(7):87-99.
- Leung, S.W., and R.L. Valentine. 1994. Unidentified Chloramine Decomposition Product - I. Chemistry and Characteristics. Water Research, 28(6):1475-1483.

- Lieu, N.I., R.L. Wolfe, and E.G. Means. 1993. Optimizing Chloramine Disinfection for the Control of Nitrification. *Journal of American Water Works Association*, 85(2):84-90.
- Liu, Suibing, Y. Chang, Michael Le Puil, James S. Taylor, A. A. Randall. 2003. NF & RO Biostability Relative to Alternative Methods of Water Treatment. Membrane Technology Conference of AWWA, 2003, Atlanta, Georgia.
- Lu, C., P. Biswas, and R.M. Clark. 1995. Simultaneous Transport of Substrates, Disinfectants and Microorganisms in Water Pipes. *Water Research*, 29(3):881-894.
- Lykins, B.W.J., W.E. Koffskey, and K.S. Patterson. 1994. Alternative Disinfectants for Drinking Water Treatment. *Journal of Environmental Engineering*, 120(4):745-758.
- McGuire, M.J. 1999. Advances in Treatment Processes to Solve Off-flavor Problems in Drinking Water. *Water Science and Technology*, 40(6):153-163.
- Metcalf and Eddy. 1991. *Wastewater Engineering, Treatment, Disposal, Reuse*, 3rd edition. McGraw-Hill, New York.
- Mitcham, R.P., M.W. Shelley, and C.M. Wheadon. 1983. Free Chlorine versus Ammonia-chlorine: Disinfection, Trihalomethane Formation, and Zooplankton Removal. *Journal of American Water Works Association*, 75(4):196-198.
- Odell, L.H., G.J. Kirmeyer, A. Wilczak, J.G. Jacangelo, J.P. Marcinko and R.L. Wolfe. 1996. Controlling Nitrification in Chloraminated Systems. *Journal of American Water Works Association*, 88(7):86-98.
- Ollos, P.J., R.M. Slawson, and P.M. Huck. 1998. Bench Scale Investigations of Bacterial Regrowth in Drinking Water Distribution Systems. *Water Science and Technology*, 38(8-9):275-282.
- Poduska, R. A., F. J. Andrews. 1974. Dynamics of nitrification in the activated sludge process. 29th Industrial Waste Conference. Purdue University, Lafayette, Indiana.
- Regan, J.M., G.W. Harrington, and D.R. Noguera. 2002. Ammonia- and Nitrite-Oxidizing Bacterial Communities in a Pilot-scale Chloraminated Drinking Water Distribution System. *Applied and Environmental Microbiology*, 68(1):73-81.
- Rittmann, B.E., and P.L. McCarty. 2001. *Environmental Biotechnology: Principles and Applications*. McGraw-Hill, New York.
- Rittmann, B.E., and V.L. Snoeyink. 1984. Achieving Biologically Stable Drinking water. *Journal of American Water Works Association*, 76(10):106-114.
- Taylor, J.S., B.R. Snyder, B. Ciliax, C. Ferraro, A. Fisher, J. Herr, P. Muller, and D. Thompson. 1984. Project Summary: Trihalomethane Precursor Removal by the Magnesium Carbonate Process. USEPA Research and Development, EPA-600/S2-84-090.
- Taylor, J.S., J.D. Dietz, S.K. Hong, L.A. Mulford, and A.A. Randall. 2001. Required Treatment and Water Quality Criteria for Distribution System Blending of Treated Surface, Ground and Saline Sources; Periodic Report 2, Applied Literature Review. University of Central Florida, Orlando.

- Thomas, J.C. 1987. M.S. Thesis: Influence of Bromide on Trihalomethane Formation and Speciation. University of Central Florida, Orlando, FL.
- Tsuno, H., T. Hidaka, and F. Nishimura. 2002. A Simple Biofilm Model of Bacterial Competition for Attached Surface. *Water Research*, 36(4):996-1006.
- Valentine, R.L. 1984. Disappearance of Monochloramine in the Presence of Nitrite. *Water chlorination: Chemistry, Environmental Impact and Health Effects*. Lewis Publ., Chelsea, Mich.
- Valentine, R.L., K.I. Brandt, and C.T. Jafvert. 1986. Spectrophotometric Study of the Formation of an Unidentified Monochloramine Decomposition Product. *Water Research*, 20(8):1067-1074.
- Vayenas, D.V., S. Pavlou, and G. Lyberatos. 1997. Development of a Dynamic Model Describing Nitrification and Denitrification in Trickling Filters. *Water Research*, 31(5):1135-1147.
- White, G. C. 1999. *Handbook of Chlorination and Alternative Disinfectants*, 4th edition. John Wiley & Sons, Inc., New York.
- Wilczak, A., J.G. Jacangelo, J.P. Marcinko, L.H. Odell, G.J. Kirmeyer and R.L. Wolfe. 1996. Occurrence of Nitrification in Chloraminated Distribution Systems. *Journal of American Water Works Association*, 88(7):74-85.
- Williamson, K., P. L. McCarty. 1976. Verification studies of the biofilm model for bacterial substrate utilization. *Journal of Water Pollution Control Federation*, 48(2):281-289.
- Wolfe, R.L., E.G. Means, M.K. Davis, and S.E. Barrett. 1988. Biological Nitrification in Covered Reservoirs Containing Chloraminated water. *Journal of American Water Works Association*, 80(9):109-114.
- Wolfe, R.L., N.I. Lieu, G. Izaguirre, and E.G. Means. 1990. Ammonia-oxidizing Bacteria in a Chloraminated Distribution System: Seasonal Occurrence, Distribution, and Disinfection resistance. *Applied and Environmental Microbiology*, 56:451-462.
- Wolfe, R.L., N.R. Ward, and B.H. Olson. 1985. Inactivation of Heterotrophic Bacterial Populations in Finished Drinking Water by Chlorine and Chloramines. *Water Research*, 19(11):1393-1403.